Nano structured Fe_2O_3 film decorated on WO_3 Nano rod for photoelectrochemical water splitting application

S. Hemapriya[1], *P. Velusamy*[1*]

[1]*Department of Physics, Thiagarajar College of Engineering, Madurai-625015, Tamil Nadu, India.*

ABSTRACT

Photoelectrochemical water splitting is an effective approach for sustainable hydrogen production and addressing global energy demands. The structure and morphology of iron oxide play a vital role in enhancing PEC performance. Fe_2O_3 possesses strong visible-light absorption, non-toxicity, earth abundance, and good chemical stability, making it a promising photoanode material. However, pristine Fe_2O_3 suffers from poor electrical conductivity due to its short hole diffusion length and high interfacial charge-transfer resistance, which limits its PEC efficiency. To overcome these limitations, Fe_2O_3 was coated on WO_3 to form a Fe_2O_3@WO_3 heterostructure, enabling improved charge separation and enhanced interfacial charge transport through favourable band alignment. In this work, nanostructured Fe_2O_3 and Fe_2O_3@WO_3 photoanodes were synthesized via a hydrothermal method to mitigate intrinsic defects and significantly improve photoelectrochemical water-splitting performance.

Key words: Photoelectrochemical, Hydrothermal, Fe_2O_3, WO_3 Nano rod, Heterojunction.

Introduction

The advancement of industry and technology made possible by fossil fuels has greatly raised human well-being. However, their limited supply and the effects of their burning on the environment demand a shift towards alternative sustainable energy sources[1]. One abundant and renewable resource that has a lot of potential to help with these issues is solar energy. The use of solar energy can be greatly increased[2,3], lowering dependency on fossil fuels and minimizing environmental degradation[4], by transforming sporadic solar energy into chemical resources that can be stored[5], like hydrogen. Photoelectrochemical water splitting technology, which is based on solar energy and water, realizes the efficient utilization of solar energy by simulating photosynthesis in nature. Under the condition of light, the solar energy is absorbed by the photoanode and the light energy is converted into electric energy. Photoelectrochemical hydrolysis device is a device that converts solar energy into chemical energy in the form of hydrogen and stores it in the form of H_2 gas. The essence of PEC hydrolysis is that under the synergistic action of photoelectricity, the chemical bond of water molecules on the surface of the catalyst is broken, and then the conversion energy of the catalyst is obtained again, and a new chemical bond is formed again. The redox reaction that occurs at each electrode is expressed by the following equation:

Cathode: $2H^{+} + 2e^{+} \rightarrow H_2$ $E^{o} = 0V$

Photoanode: $2H_2O + 4h^{+} \rightarrow O_2 + 4h^{+}$ $E^{o} = 1.23V$

According to the above equation, we can know that the minimum voltage of photoelectrochemical hydrolysis is 1.23V. Therefore, the theoretical minimum energy of an electron excited should be 1.23eV. In order to meet this requirement, the energy absorbed by the photoelectrode must be greater than or equal to the energy of 1.23eV [6]. But in fact, due to the energy loss, the energy absorbed by photons should be much larger than the theoretical value. In order to achieve spontaneous photoelectrochemical hydrolysis, it is of great significance to improve the efficiency of photoelectrochemical hydrolysis by improving the defects of semiconductor materials. The photoanode is usually a semiconductor material, that is, when the near surface region of the semiconductor is exposed to light radiation whose energy is greater than its band gap energy, the electrons in the valence band will be excited and transition to the conduction band, Because of the band gap in semiconductors, the relaxation process of excited electrons is much slower than that of excited electrons in metals. High-energy light excitation can produce electron-hole pairs in semiconductors, that is, semi-materials produce electron-hole pairs by absorbing light. The photoanode and the cathode form a photoelectrochemical cell. After the photoanode absorbs light under the action of an external electric field, the electrons generated on the semiconductor strip migrate to the cathode through the external circuit, and the protons in the water receive the redox reaction of hydrogen production from the cathode

PEC water splitting is one of the most promising methods for producing hydrogen[7]. One interesting method for producing green H_2 is photoelectrochemical (PEC) water splitting. Unlike solar cell-powered electrocatalysis, PEC is still distant from commercialization despite its benefits, such as the combination of light absorption and gas evolution on the same material surface[8,9]. Because of their exceptional chemical and operational stability under ambient settings, metal oxides (such as TiO_2, CuO, WO_3 and Fe_2O_3) are among the most extensively researched materials for electrochemical applications[10,11]. To create photoactive semiconductors with large surface areas appropriate for energy conversion applications, a number of well-established techniques are used, such as electrodeposition, sol-gel processing, and solvothermal synthesis[12,13]. By applying a suitable voltage/current density in a suitable electrolyte, anodic oxidation, also known as anodization, is a simple and scalable method for creating nanostructured metal oxides directly on the surface of their corresponding metals. This technique reduces difficulties related to adhesion to substrate during direct material development and does away with the necessity for extra coating stages needed for powders[14]. The concentrate on WO_3, a thoroughly researched narrow band gap photoanode material with a valance band maximum appropriate for water oxidation, moderate electron mobility (far higher than that of Fe_2O_3), and stability in acidic conditions. However, WO_3 exhibits a low light absorption coefficient, which necessitates the use of thicker layers for sufficient light harvesting – this, in turn, increases the likelihood of unwanted recombination of photogenerated electron-hole pairs before they can participate in water splitting reactions[15]. In the context of porous WO_3 production, anodic oxidation of tungsten has been thoroughly described in the literature[16]. Additionally, it was demonstrated that the deposition of appropriate co-catalysts might improve its photoelectrochemical performance. However, tungstates are difficult to use as overlayers in photoanodes illuminated from the photoactive material side (front illumination), especially when grown on opaque metal substrates, because they usually show narrower band gaps than WO_3 [17]. In fact, there aren't many examples of co-catalyst deposition on anodized WO_3 electrodes because these layers might prevent light from getting to the photo absorber. Nonetheless, various effective methods have been demonstrated to improve the photoelectrochemical water oxidation performance of anodic WO_3 [18]. We have decided to investigate Fe_2O_3, for which there are no prior reports on the deposition of a pure phase on WO3 electrode, regardless of the synthesis or coating technique for PEC water splitting, in order to fill this crucial research gap in co-catalyst decorated anodic WO_3 photoelectrodes. The hydrothermal approach has been used for the synthesis of Fe_2O_3 nanoparticles because it provides single-phase polycrystalline powder synthesis at a moderate temperature, which is required for predictable optical and electrical properties [19,20]. In this study the coating of Fe_2O_3 coated on WO_3 for water splitting application in FTO is analysed from EIS study.

Experiment

The material used in synthesis process initiate with FTO substrate with the resistance of 14 Ω, square and thickness of glass 5cm×1.0cm×0.16cm. Ammonium oxalate ($(NH_4)_2C_2O_4.H_2O$), Sodium tungstate ($Na_2WO_4.2H_2O$), Hydrochloric acid (HCl), Sodium nitrate ($NaNO_3\cdot 6H_2O$), Ferric trichloride ($FeCl_3$), Nickel nitrate ($Ni(NO_3)_2\cdot 6H_2O$), ferric nitrate ($Fe(NO_3)_3\cdot 9H_2O$), urea, Na_2SO_4.

Synthesis of WO_3 Films and WO_3 Nano rods begins with hydrothermal method. Typically, 0.1237 g sodium tungsten dehydrates ($Na_2WO_4.2H_2O$) was dissolved in 15 mL of distilled water as solution A, 0.1172 g ammonium oxalate ($(NH_4)_2C_2O_4\ H_2O$) was added into 15 mL of distilled water as a solution B. 5ml of HCl solution (3.0 M) was slowly dropped into solution A. After stirring few minutes at room temperature, the white suspension was obtained. The solution B was then added into suspension. When the suspension became clear, the mixture was moved into a 50 mL of the stainless autoclave, the FTO glass was placed vertically to the bottom of the Teflon-lined stainless-autoclave and conducting side facing down was immersed, then sealed and thermally treated at 140 °C for 6 h. Afterward, the obtained samples were washed thoroughly and dried in air overnight at 60 °C. The products were calcined at 500 °C for 2.5 hr to obtain the WO_3 films.

After synthesis of WO_3 nanorods, $Fe_2O_3@WO_3$ Heterojunction is prepared by hydrothermal method. Specifically, 0.87 g ferric trichloride ($FeCl_3.6H_2O$) was slowly dissolved in 30 mL of distilled water, 0.5099 g sodium nitrate ($NaNO_3.6H_2O$) was then added into the mixture. After a few minutes of stirring the mixture was placed into a 50 mL stainless autoclave in which immersed FTO substrate with WO_3. The autoclave was maintained at 100 °C for 6 h. After the reaction, the obtained samples were washed thoroughly using distilled water and absolute alcohol followed by drying at 60 °C in the air. Finally, the obtained products were calcined at 600 °C for 2 hr.

Result & Discussion

XRD

The crystal structure and phase purity of the synthesized materials are analyse using X-ray diffraction (XRD) shows in Fig.1. The XRD pattern exhibits distinct diffraction peaks at 2θ values of 24.4°, 26.6°, 35.8°, 38.0°, and 51.7°, which are indexed to the (106), (116), (119), (209), and (329) crystallographic planes respectively. These diffraction peaks are perfect match with the standard data reported in the JCPDS card No. 00-015-0615, confirming the formation of tetragonal phase Fe_2O_3. The crystalline structure of the synthesized WO_3 shows prominent diffraction peaks at 2θ values of 23.7°, 24.2°, 34.0°, 34.8°, 37.9°, 44.2°, 50.5°, and 56.5°, which are indexed to the (002), (200), (220), (–212), (–103), (320), (–114), and (1–24) crystallographic planes, respectively. These diffraction peaks closely match the standard data of WO_3 as per the JCPDS card No. 00-002-0310. The analysation of XRD of Fe_2O_3@WO_3 visualise the presenting of both WO_3 and Fe_2O_3 by identify their diffraction indexes in the resulted peaks.

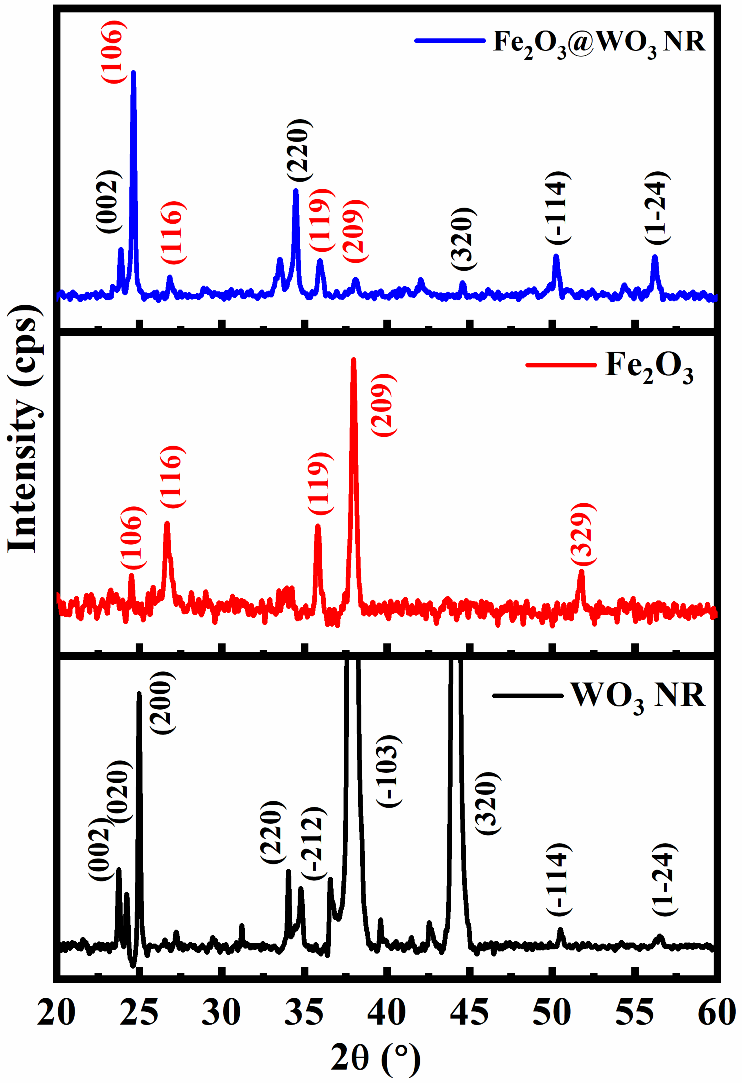

Fig.1. XRD patters of WO_3 Nano rod, Fe_2O_3 and Fe_2O_3@ WO_3 nano structured photoanode

SEM

In thin film the coated substrates are undergoes Scanning Electron Microscopy (SEM) to examine the surface coverage, thickness uniformity, and adhesion of material. WO_3 shown in Fig.2. which is known for its structural versatility, commonly existing in monoclinic, orthorhombic, and hexagonal phases depending on temperature. The WO_3 nanorod formation is confirm the existence of the central tungsten atom is surrounded by oxygen atoms. In Fig.3. the formation of nanoparticles od Fe_2O_3 are clearly visualised. The structure consists of an hcp (hexagonal close-packed) array of oxygen anions (O^{2-}) with Fe^{3+} ions occupying two-thirds of the octahedral interstices. The heterojunction structure of Fe_2O_3@WO_3 composite material where the two oxides are brought into contact shown in Fig.4. This is typical core-shell structure which shows highly integrated heterostructure. There is a transition in lattice fringes which represent the interface between atomic planes. This structure is engineered to improve photocatalytic property.

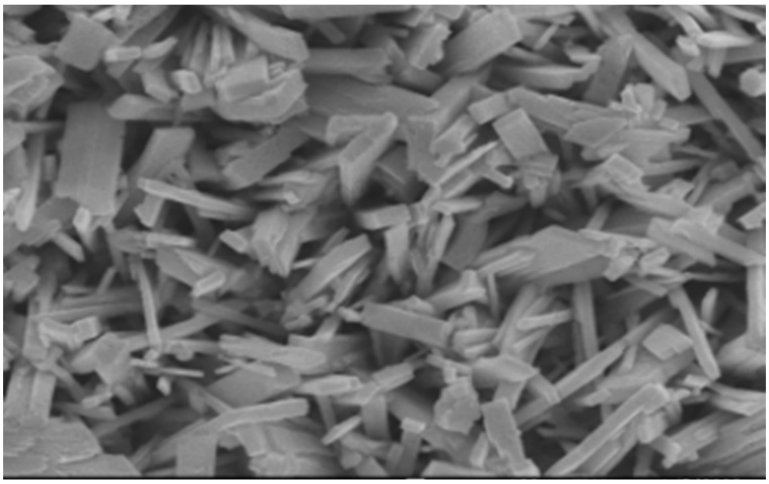

Fig. 2. SEM image of WO_3 Nano rod

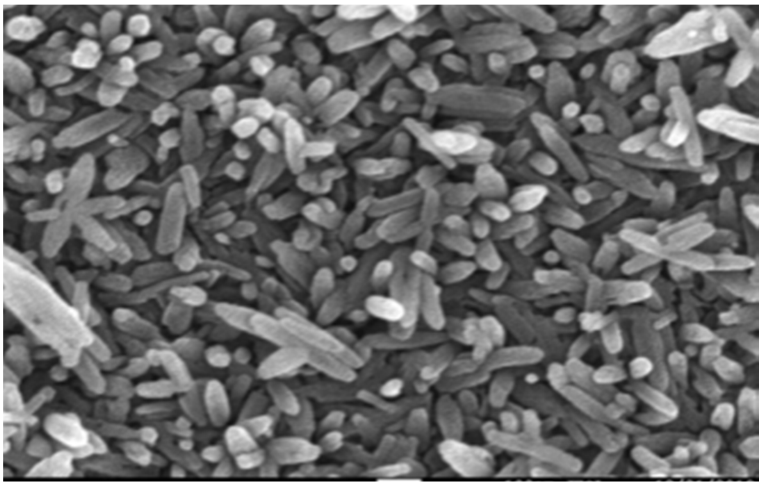

Fig. 3. SEM image of Fe_2O_3 Nano structure

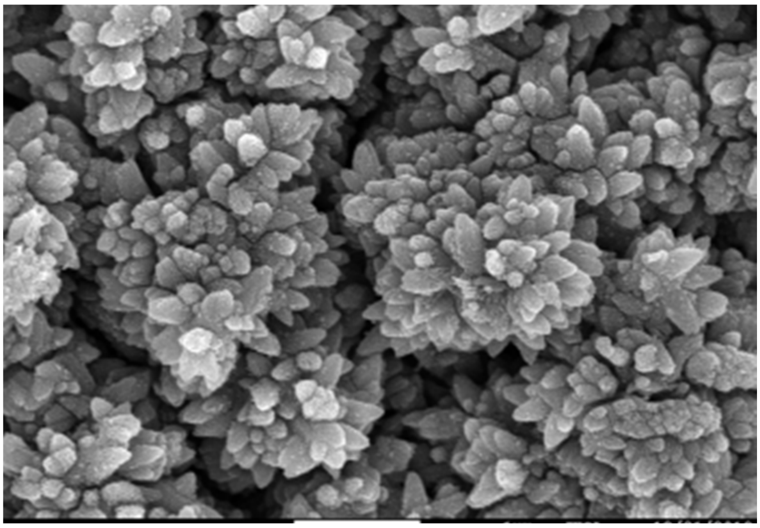

Fig. 4. SEM image of Fe_2O_3 @WO_3 Nano rod

EIS

Electrochemical Impedance Spectroscopy (EIS) analysis was carried out to evaluate the charge-transfer kinetics of the electrode for water-splitting applications in Fig.5. The Nyquist plot of Fe_2O_3@WO_3 exhibits a depressed semicircle in the high-frequency region followed by a straight line in the low-frequency region, indicating a combination of charge-transfer resistance and diffusion-controlled processes. The smaller semicircle diameter suggests a low charge-transfer resistance (Rct) at the electrode–electrolyte interface, confirming enhanced electrical conductivity and faster electron transport. This improved interfacial charge transfer facilitates efficient electrocatalytic reactions during the hydrogen and oxygen evolution processes. The inclined line at lower frequencies reflects favourable ion diffusion and capacitive behaviour, which further supports sustained electrochemical activity. Overall, the EIS results demonstrate that the electrode possesses excellent charge-transfer characteristics, making it a promising candidate for efficient water-splitting applications.

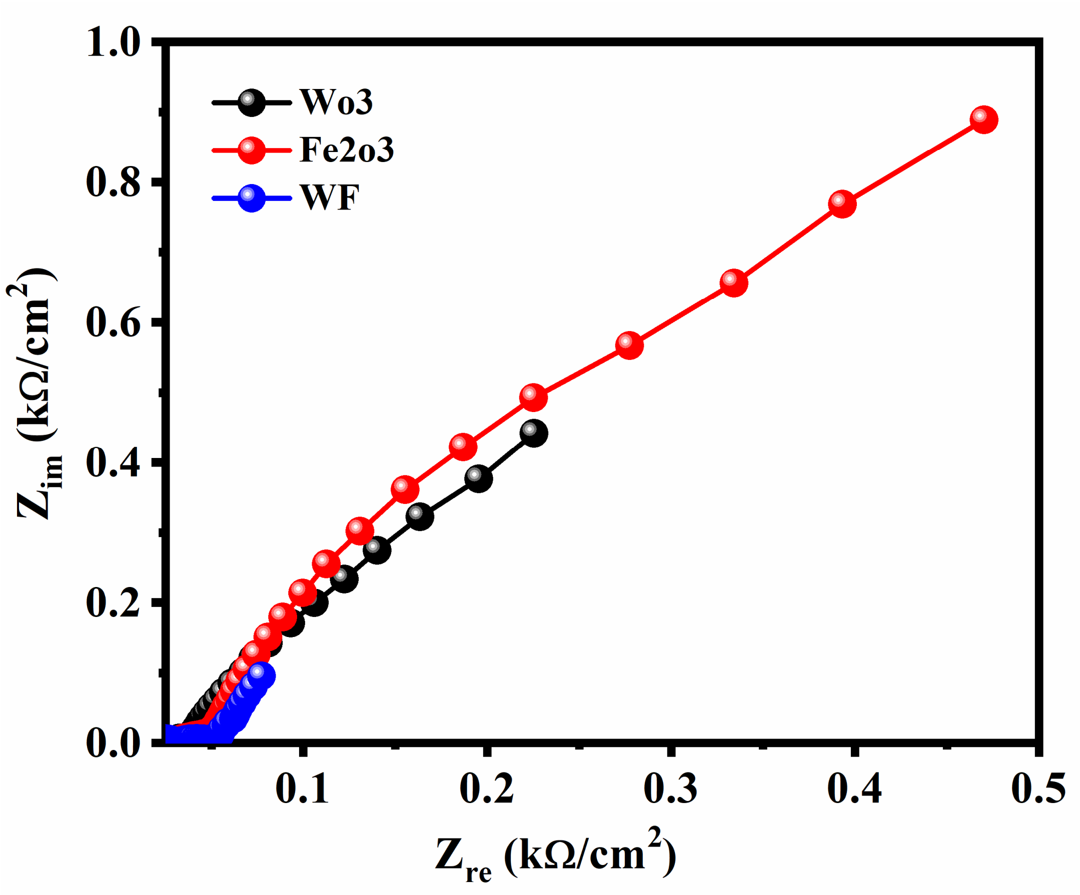

Fig. 5. EIS curve of Fe_2O_3@WO_3 photoanode

Conclusion:

The nanostructured Fe_2O_3, WO_3 nanorods, and Fe_2O_3@WO_3 composite were successfully synthesized via a hydrothermal method. X-ray diffraction analysis confirmed the formation of well-defined polycrystalline phases of Fe_2O_3, WO_3, and Fe_2O_3@WO_3 without the presence of secondary impurities. FE-SEM studies revealed that the additive played a significant role in modifying the surface microstructure of Fe_2O_3, resulting in distinct nanostructured morphologies. Surface morphology analysis showed that WO_3 exhibited flake-like nanorod structures, while Fe_2O_3 formed uniform nanorods, providing a large surface area and abundant electroactive sites. Electrochemical impedance spectroscopy demonstrated that the Fe_2O_3@WO_3 composite exhibited the smallest semicircle diameter, indicating a markedly reduced charge-transfer resistance and improved interfacial electron transport. The enhanced electrical conductivity and synergistic interaction between Fe_2O_3 and WO_3 significantly promote charge-transfer kinetics. These results confirm that the rational design of additive-assisted heterostructure nanomaterials is an effective strategy for improving electrochemical performance. Consequently, the synthesized nanostructures show strong potential water-splitting applications.

Acknowledgement:

The author S. Hemapriya sincerely thank TCE for its financial support under the Thiagarajar Research Fellowship plan (File no.: TCE/RD/TRF/<<10>> dated 27.09.2024).

Reference

(1) Ng, K. H.; Lai, S. Y.; Cheng, C. K.; Cheng, Y. W.; Chong, C. C. Photocatalytic Water Splitting for Solving Energy Crisis: Myth, Fact or Busted? *Chem. Eng. J.* **2021**, *417*, 128847. https://doi.org/10.1016/j.cej.2021.128847.

(2) Herron, J. A.; Kim, J.; Upadhye, A. A.; Huber, G. W.; Maravelias, C. T. A General Framework for the Assessment of Solar Fuel Technologies. *Energy Environ. Sci.* **2014**, *8* (1), 126–157. https://doi.org/10.1039/C4EE01958J.

(3) Feng, C.; Li, Y. Self-Healing Mechanisms toward Stable Photoelectrochemical Water Splitting. *Chin. J. Catal.* **2024**, *60*, 158–170. https://doi.org/10.1016/S1872-2067(23)64648-0.

(4) Gondal, I. A. Offshore Renewable Energy Resources and Their Potential in a Green Hydrogen Supply Chain through Power-to-Gas. *Sustain. Energy Fuels* **2019**, *3* (6), 1468–1489. https://doi.org/10.1039/C8SE00544C.

(5) Tabah, B.; Pulidindi, I. N.; Chitturi, V. R.; Arava, L. M. R.; Varvak, A.; Foran, E.; Gedanken, A. Solar-Energy-Driven Conversion of Biomass to Bioethanol: A Sustainable Approach. *J. Mater. Chem. A* **2017**, *5* (30), 15486–15506. https://doi.org/10.1039/C7TA03083E.

(6) *Photoelectrochemical Water Splitting by Using Nanomaterials: A Review | Journal of Electronic Materials | Springer Nature Link.* https://link.springer.com/article/10.1007/s11664-023-10794-z (accessed 2026-01-30).

(7) Yang, H.; Li, S.; Yu, S.; Yu, X.; Zhao, H.; Wang, C.; Ping, D.; Zheng, J. Y. Strategies for Enhancing the Stability of WO3 Photoanodes for Water Splitting: A Review. *Chem. Eng. Sci.* **2025**, *302*, 120894. https://doi.org/10.1016/j.ces.2024.120894.

(8) *Hole utilization in solar hydrogen production | Nature Reviews Chemistry.* https://www.nature.com/articles/s41570-022-00366-w (accessed 2026-01-30).

(9) Ng, W. C.; Yaw, C. S.; Shaffee, S. N. A.; Samad, N. A. A.; Koi, Z. K.; Chong, M. N. Elevating the Prospects of Green Hydrogen (H2) Production through Solar-Powered Water Splitting Devices: A Systematic Review. *Sustain. Mater. Technol.* **2024**, *40*, e00972. https://doi.org/10.1016/j.susmat.2024.e00972.

(10) Abdullah, R.; Jalil, A. A.; Asmadi, M.; Hassan, N. S.; Bahari, M. B.; Alhassan, M.; Izzudin, N. M.; Sawal, M. H.; Saravanan, R.; Karimi-Maleh, H. Recent Advances in Zinc Oxide-Based Photoanodes for Photoelectrochemical Water Splitting. *Int. J. Hydrog. Energy* **2025**, *107*, 183–207. https://doi.org/10.1016/j.ijhydene.2024.05.461.

(11) Niu, H.; Gao, L.; Liu, M.; Zou, Y.; Wang, J.; Hu, G.; Jin, J. Rapid Charge Extraction via Hole Transfer Layer and Interfacial Coordination Bonds on Hematite Photoanode for Efficient Photoelectrochemical Water Oxidation. *Appl. Catal. B Environ. Energy* **2024**, *358*, 124369. https://doi.org/10.1016/j.apcatb.2024.124369.

(12) Syrek, K.; Zych, M.; Pisarek, M.; Gondek, Ł.; Gurgul, M.; Palowska, R.; Liu, L.; Sulka, G. D. Novel Anodic WO3-SeO2-CuO Photoelectrode Operating under Solar Illumination for Water-Splitting Applications. *J. Power Sources* **2025**, *640*, 236656. https://doi.org/10.1016/j.jpowsour.2025.236656.

(13) *Photoelectrocatalytic degradation of glyphosate on titanium dioxide synthesized by sol-gel/spin-coating on boron doped diamond (TiO2/BDD) as a photoanode - ScienceDirect*. https://www.sciencedirect.com/science/article/abs/pii/S0045653521009589?via%3Dihub (accessed 2026-01-30).

(14) Mohapatra, B. D.; Sulka, G. D. Review of Anodic Tantalum Oxide Nanostructures: From Morphological Design to Emerging Applications. *ACS Appl. Nano Mater.* **2024**, *7* (12), 13865–13892. https://doi.org/10.1021/acsanm.4c02000.

(15) Penkova, Y.; Betova, I.; Karastoyanov, V.; Bojinov, M. Electrochemical Synthesis and Characterization of Tungsten Oxide Catalysts for Photoelectrochemical Water Splitting. *Electrochimica Acta* **2024**, *480*, 143908. https://doi.org/10.1016/j.electacta.2024.143908.

(16) Zych, M.; Syrek, K.; Pisarek, M.; Sulka, G. D. Synthesis and Characterization of Anodic WO3 Layers *in Situ* Doped with C, N during Anodization. *Electrochimica Acta* **2022**, *411*, 140061. https://doi.org/10.1016/j.electacta.2022.140061.

(17) *Transition metal tungstates AWO4 (A2+ = Fe, Co, Ni, and Cu) thin films and their photoelectrochemical behavior as photoanode for photocatalytic applications | Journal of Applied Electrochemistry | Springer Nature Link*. https://link.springer.com/article/10.1007/s10800-023-01851-w (accessed 2026-01-30).

(18) Patil, A. R.; Dongale, T. D.; Pedanekar, R. S.; Sutar, S. S.; Kamat, R. K.; Rajpure, K. Y. Multilevel Resistive Switching in Hydrothermally Synthesized FeWO4 Thin Film-Based Memristive Device for Non-Volatile Memory Application. *J. Colloid Interface Sci.* **2024**, *669*, 444–457. https://doi.org/10.1016/j.jcis.2024.04.222.

(19) Patil, A. R.; Dongale, T. D.; Pedanekar, R. S.; Sutar, S. S.; Kamat, R. K.; Rajpure, K. Y. Multilevel Resistive Switching in Hydrothermally Synthesized FeWO4 Thin Film-Based Memristive Device for Non-Volatile Memory Application. *J. Colloid Interface Sci.* **2024**, *669*, 444–457. https://doi.org/10.1016/j.jcis.2024.04.222.

(20) Chatterjee, P.; Piecha, D.; Szczerba, M.; Marzec, M. M.; Pisarek, M.; Uchacz, T.; Sulka, G. D. Enhanced Photoelectrochemical Water Splitting Activity of Porous Anodic WO3 Photoelectrodes Decorated with FeWO4 Nanoparticles. *Mater. Des.* **2025**, *260*, 115018. https://doi.org/10.1016/j.matdes.2025.115018.

Abstract

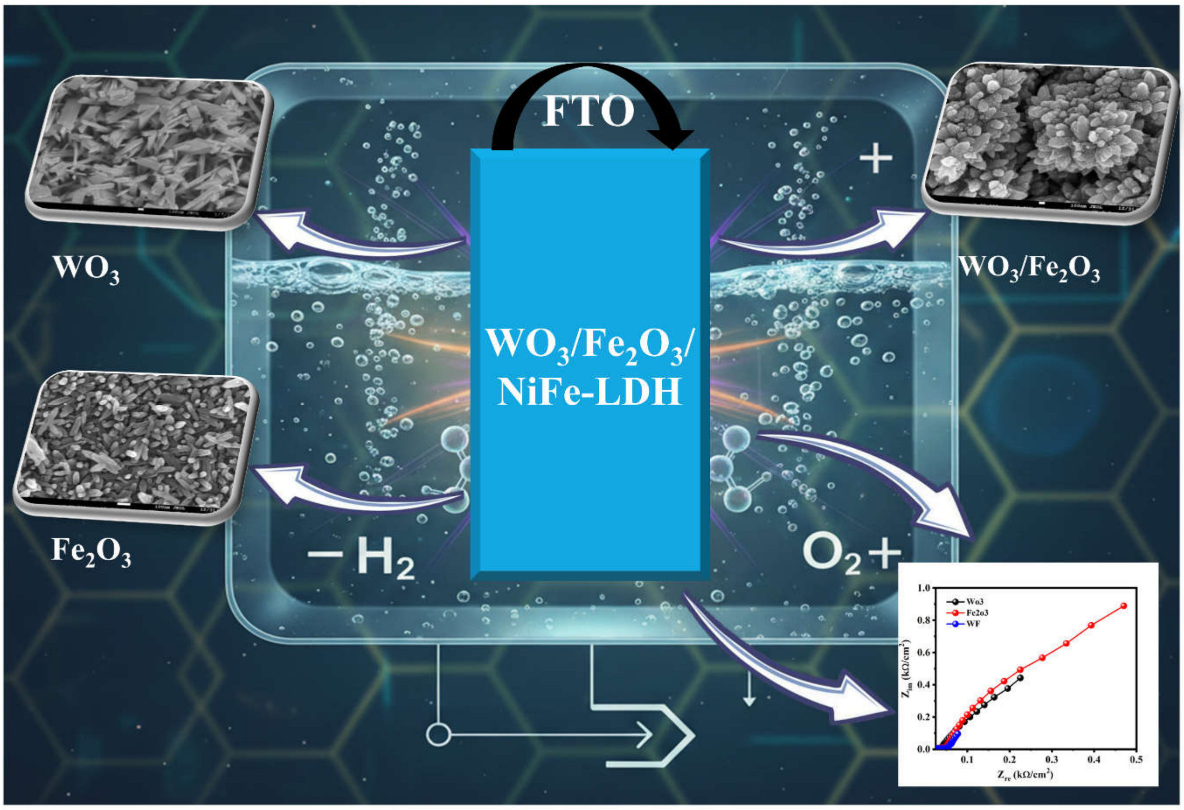
FTO
WO_3
WO_3/Fe_2O_3
+
$WO_3/Fe_2O_3/$ NiFe-LDH
Fe_2O_3
$-H_2$
O_2+
1.0
0.8
0.6
0.4
0.2
0.0
Wo3
Fe2o3
WF
Z_{im} (kΩ/cm^2)
0.1
0.2
0.3
0.4
0.5
Z_{re} (kΩ/cm^2)